Voltage-Controlled Magnetic Tunnel Junctions Demonstrate Resilience to Displacement Damage

Christopher H. Bennett[1] *Member, IEEE*, T. Patrick Xiao[1] *Member, IEEE*, Romney R. Katti[2], *Senior Member, IEEE*, Joshua Young[1], *Member, IEEE*, Yixin Shao[3], Jordan G. Athas[3], Pedram Khalili Amiri[3], Noraica Davila-Melendez[4], Goran Mihajlovic[4], Jordan A. Katine[4], Ed Bielejec[1] *Member, IEEE*, and David R. Hughart[1] *Member, IEEE*

[1]Sandia National Laboratories, Albuquerque, NM, USA
[2]Honeywell Aerospace, Minneapolis, MN, USA
[3]Northwestern University, Evanston, IL, USA
[4]Western Digital, San Jose, CA, USA

Abstract – Magnetic tunnel junctions (MTJs) with voltage-controlled magnetic anisotropy properties were electrically profiled and irradiated with 20 MeV Au ions. At high fluences tunneling magnetoresistance and coercivity degrade, matching the response of standard perpendicular anisotropy MTJs.

Keywords – spintronics, magnetic tunnel junctions, displacement damage, heavy ion irradiation, voltage-controlled magnetic anisotropy, post-CMOS logic

Corresponding (and presenting) author:

CH Bennett, Sandia National Laboratories, 1515 Eubank Blvd SE, MS-1084, Albuquerque, NM 87123, USA, phone: 505-239-1680, email: cbennet@sandia.gov

Contributing authors:

T.P. Xiao, J. Young, E. Bielejec, and D. Hughart are with Sandia National Laboratories, Albuquerque, NM 87185

R.R. Katti is with Honeywell Aerospace, Minneapolis, MN, 55413

Y. Shao, J. Athas, and P. K. Amiri are with Northwestern University, Evanston, IL, 60208

N. Davila-Melendez, G. Mihajlovic, and J. Katine are with Western Digital, San Jose , CA, 95119

Presentation Preference: Oral Presentation

Session Preference: Basic Mechanisms

Sandia National Laboratories is a multimission laboratory managed and operated by National Technology and Engineering Solutions of Sandia, LLC, a wholly owned subsidiary of Honeywell International, Inc., for the U.S. Department of Energy's National Nuclear Security Administration under contract DE-NA0003525.

***Abstract*—Several magnetic tunnel junctions with voltage-controlled magnetic anisotropy (VCMA) properties were electrically profiled and subjected to microbeam irradiation. The microbeam allows for precise analysis of fluence's effect on the device's switching ratio (tunneling magnetoresistance (TMR)) and magnetic field response (coercivity). The devices are resilient to 20MeV Au ion fluences up to $1 \times 10^{12}\,\mathrm{ion/cm^2}$ Beyond this, they show electrical differences, specifically, a strong negative correlation between applied fluence and TMR, and a weak negative correlation for coercivity. Additionally, we find that the devices fit tightly to the displacement damage response of previously analyzed perpendicular anisotropy MTJs. This work confirms that these promising next-generation logic or neuromorphic device candidates are similarly radiation-resilient as other species of MTJs.**

I. Introduction

MAGNETIC tunnel junctions are a promising memory device candidate for systems featuring the tight integration of logic and memory. In contrast to other experimental devices that have unproven characteristics, MTJs possess extreme write/read endurance, easy CMOS compatibility, high yield, and instant-on-off behavior [1]. Recently, voltage controlled magnetic anisotropy (VCMA) has been explored as a fundamental way to yield multi-functionality from the basic MTJ crystalline physics [2]. VCMA effects could significantly enhance the energy efficiency and capability of systems executing MTJ-based logic [3], probabilistic computing [4], and hardware locking [5]. Another advantage of MTJs is that they are intrinsically radiation-hard, being non-charge-driven switching devices; this has been broadly confirmed in the literature [6]–[8].

However, to our knowledge, analysis of the radiation resilience of perpendicular anisotropy MTJs with VMCA capabilities has not been discussed in the literature. Notably, VCMA pMTJs have a different material stack and material optimizations than standard pMTJs, and may therefore be intrinsically more sensitive to induced damage. In this work, we evaluate the radiation response of this emerging device class to heavy ion effects, which are notably effective at inducing observable in emerging MTJ devices.

II. Methodology

The devices studied in this work have a stack similar to [9]. The perpendicular magnetic tunnel junction devices (pMTJs), which have a VCMA coefficient of up to 130 fJ/Vm, are nanopillars of various diameters: 30nm, 50nm, and 70nm. The thin film stacks were sputter-deposited in an ultra-high vacuum (UHV) physical vapor deposition (PVD) system (Canon ANELVA HC7100), and annealed at wafer level for 30 min at 400°C before patterning and device fabrication. As described in [9], the studied pMTJs allow for voltage-modulated switching in the sub-volt region. Specifically, the devices are highly sensitive to the voltage applied, which has differential effects on tunneling magnetoresistance (TMR) and coercivity (width of the magnetic field hysteresis loop). Specifically, negative voltages approaching -1V minimize the coercivity of the field loop, and positive voltages approaching 1V maximize the coercivity of the field loop. In contrast,

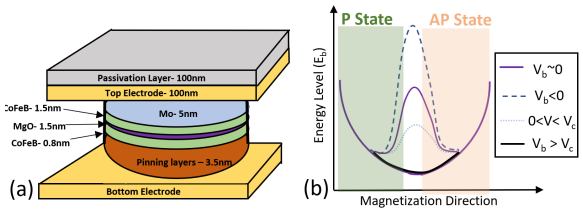

Fig. 1. (a) Stack of studied VCMA pMTJs. (b) In a pMTJ with VCMA, the energy barrier between the parallel (P) and anti-parallel (AP) states can be modulated by an applied voltage. Figure is inspired by similar cartoon in [2].

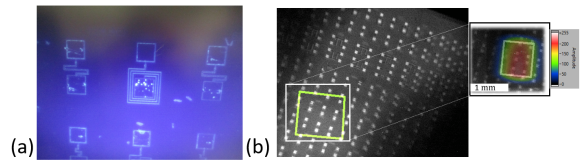

Fig. 2. (a) Microscope image of device pads during electrical probe pre-rad measurements. (b) Microscope image during ion-beam irradiation at the QASPR-III end station. As visible, beam can be rastered to the specific target location and precise calculations of fluence applied can be made.

large voltages minimize the TMR, whereas small voltages approaching 0V maximize the TMR. Lastly, negative V_b leads to the largest increase E_b, and specifically, small negative voltages lead to the highest possible TMR, as in Fig. 1(b). As pictured, bias voltages V_b change the energy barrier of the device, making switching easier (low E_b) or harder (high E_b). As given in [2], E_b depends on voltage as:

$$E_b\left(V_b\right) \approx \left[K_i\left(V_b\right) - 2\pi M_s^2\left(N_z - N_{x,y}\right) t_{fl}\right] \cdot A \quad (1)$$

Thus, energy barrier modulation occurs via modification of the interfacial perpendicular magnetization anisotropy (PMA) term (K_i), but is also critically affected by other parameters (e.g., saturation magnetization M_s), and device geometry factors (area A, and free layer thickness t_{fl}). Here, the interfacial PMA term has been carefully maximized in multiple ways; the inert nature of the Mo cap layer, and the specific Boron concentrations chosen in the active layer, each play a role as discussed in [9]. The VCMA coefficient can be derived if the energy barrier at zero bias voltage is known:

$$\frac{E_{\mathrm{b}}(V_b)}{D^2} = \frac{\xi\pi}{4t_{\mathrm{MgO}}} V_b + \frac{E_{\mathrm{b}}(V_b = 0)}{D^2} \quad (2)$$

Where ξ is the VCMA coefficient. In the studied devices, ξ varies between 100 and 40 fJ/Vm, with smaller devices having a higher coefficient. Empirically obtaining ξ depends on observation of the spontaneous relaxation at near zero-bias. In our electrical analysis, we focused instead on larger fingerprints of VMCA effect, as described next.

A. Electrical characterization

Initially, $n = 22$ devices were electrically profiled, with two devices designated as controls. Of the initial pool, three devices became open and/or shorted due to pad contacting issues (including a control), and six devices became open after

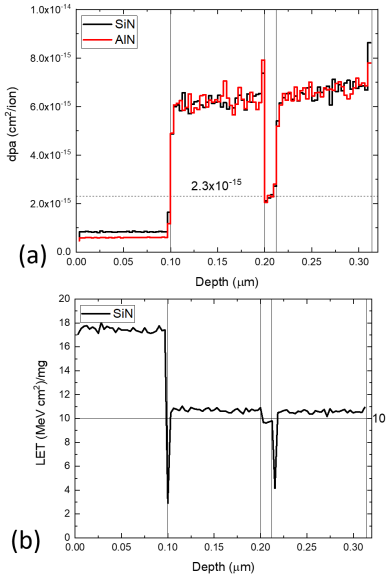

Fig. 3. (a) Induced displacement per atom as a function of depth given the stack shown in Fig. 1(a) using the Au microbeam; (b) equivalent linear energy transfer (LET) generated by the Au ions also as a function of depth.

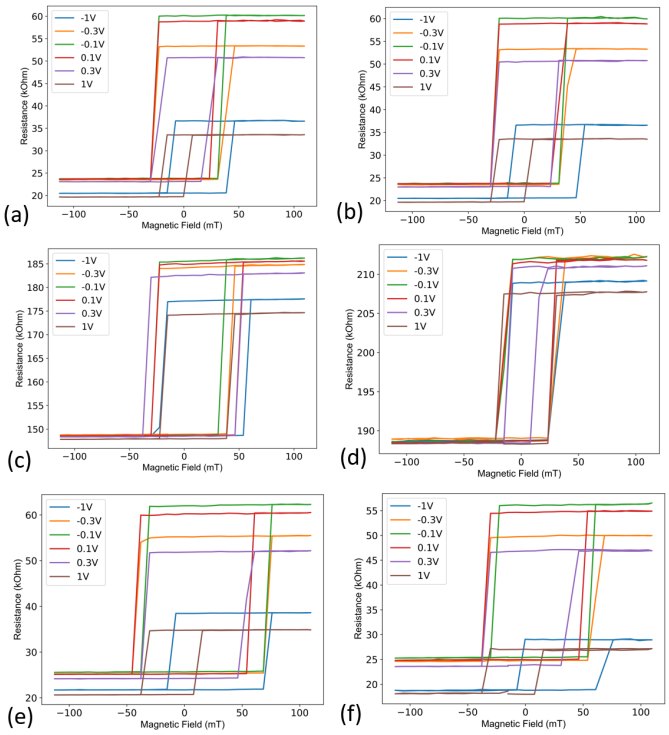

Fig. 4. (a) Pre-irradiation outer loops for the control device (QS1). (b) Post-irradiation for the control device. (c) Pre-irradiation outer-loops for an example QS2 device; (d) Outer loops for this same device post fluence $2.18\times10^{12}\,\mathrm{ion/cm^2}$. (e) Same curves for an example QS1 device. (f) Change in curves following a total fluence of $2.31\times10^{12}\,\mathrm{ion/cm^2}$.

exposure to large Au fluences. While pulse-based switching methods may be preferable for physics applications, to obtain a core fingerprint that was both electrically expressive and quick to run in between irradiation events, we conducted a set of outer-loop sweeps. In these loops, the device was ranged over a set of magnetic fields while individual I/V curves were executed at various values of V_b, specifically: $V_b = -1\mathrm{V} - 0.3\mathrm{V}, -0.1\mathrm{V}, 0.1\mathrm{V}, 0.3\mathrm{V}, 1\mathrm{V}$. An example of these loops for pre-tested devices, including two later irradiated devices and the control, are shown in Fig. 4(a), (c), (f). In order to yield field measurements, an electromagnet below the devices with precise current-based control was used to exercise a field upon the devices during electrical measurements. The electromagnet generates a perpendicular field of up 0.5T at $z = 5mm$ height, which can be read with a precise sensor in real-time.

During our pre-test, it became clear that the chip contained pMTJ VCMA parts of various quality classes. While all $n = 13$ of our profiled bits showed at least some VMCA effect, there was a distinction between high-quality pMTJ VCMA bits that showed curves very similar to those highlighted in [9], and devices that showed minor but still significant changes in both TMR and coercivity (H_c) as a function of applied voltage. An example of an irradiated device in each of the two classes is shown in Fig 4. (e),(f) and (c),(d), respectively. We divided the studied final 13 devices into a quality set 1 (QS1) of $n = 6$ devices, which included the control, and a quality set 2 (QS2) of $n = 7$, with the following two qualitative metrics helping define the difference:

- QS1 devices showed a major range difference between field loops at high V_b and low V_b states; the former showing only a small overlap with the latter. Contrarily, QS2 devices showed significant overlap between the VMCA states, albeit with some change.
- QS1 devices showed a greater than $2\times$ jump in coercivity (H_c) as a function of field, especially between the max positive voltage $V_b = 1\mathrm{V}$ and the min negative voltage $V_b = -1\mathrm{V}$. QS2 devices showed a much smaller change.

B. Displacement damage experimental design

In order to study the interfacial physics of the VCMA pMTJ devices, a heavy ion micro-beam was used to create microscopic defects within the material stacks of 12 devices. The heavy ion species and beam energy, a $20\,(\mathrm{MeV}$ Au microbeam, was chosen after conducting Stopping and Range of Ions in Matter (SRIM) calculations [10] based on the device depth profile and with the goal of concentrating damages within the active layer areas (specifically, between the Mo capping layer and the SAF layers). As visible in Fig. 3(a), the displacements per atom (dpa) from the Au ions are estimated as around $2.3\times10^{-15}\,\mathrm{cm^2/ion}$ in this region, following the stack information provided. In addition, we have estimated the effective linear energy transfer (LET) as between $5\,(\mathrm{MeVcm^2})/\mathrm{mg}$ and $10\,(\mathrm{MeVcm^2})/\mathrm{mg}$ within the active layer region of interest. All experiments were conducted in the QASPR-III (Q3) chamber at Sandia's Ion Beam Laboratory. As visible in Fig. 2(b), the Q3 end chamber allows for precise targeting of the microbeam, as well as precise calculation of the device-by-device fluence and dpa effectuated per pulse.

III. Response to Microbeam Irradiation

A. Device behavioral response

Overall, our exposed pMTJ VCMA devices saw very minor changes in either coercivity or TMR when the ion fluence was less than $1 \times 10^{12}\,\mathrm{ion/cm^2}$, but increasingly obvious changes in the magnetic field loop between that threshold and the limit of fluence we reached $4 \times 10^{12}\,\mathrm{ion/cm^2}$. Examples of these changes are shown in Fig. 4(d) and (f). As visible, both TMR and coercivity characteristically become reduced, with the changes being more noticeable on the sensitive low V_b bias levels where the VCMA effect is most expressive initially.

B. Population statistics of the ion irradiation response

To make more rigorous claims about the ion-induced changes in both TMR and coercivity H_c as a function of applied fluence, a statistical analysis was conducted. The total number of analyzed datapoints is $n = 18$, since 6 devices were measured twice (hit by the microbeam two different days at two different levels). All device exposure datapoints were normalized, *e.g.* divided by their pre-radiation value , in order to reduce the outsized impact of variance between devices when conducting regression, since the inter-sample starting values of both TMR and H_c were high . For instance, starting mean for $V_b = -1$ across all devices was TMR = 38, with a standard deviation of $\sigma = 11.1$; the highest values at $V_b = -0.1$ averaged as TMR = 72 with a standard deviation of f $\sigma = 15.2$ Meanwhile, at the highest coercivity values $V_b = -1$, mean was $H_c = 75mT$ and $\sigma = 19.3mT$, and at the lowest $V_b = 1$, mean was $H_c = 49.6mT$ and $\sigma = 15.7mT$. Within these normalized populations, we applied linear regression fits to the data points to understand the strength and slope of fluence dependence of the two parameters at each bias voltage.

As visible in Fig 5(a),(b), there is a weak and strong dependence of change in normalized coercivity and normalized TMR respectively on fluence, respectively. In the case of coercivity, linear regression yielded gentle slopes for all 6 bias voltage subsets of the data, and only 3 of the 6 levels were considered to have a statistically significant trend (denoted as * in Table 1). We attribute this at least in part to the coarseness of our field sweeps conducted ($\Delta = 8mT$ between individual points along the field loops), so that any level of stochasticity of the field response on either side of the hysteresis curve can result in $8 - 16mT$ swings before radiation. Regardless, the width of many field loops are only gently changed at high fluence values, with a few notable exceptions , such as $V_b = -1V$, where the effect is visually evident in almost all cases (see changes between Fig 4.(e),(f)).

In contrast, the dependence of TMR on applied fluence is highly statistically significant in all cases (denoted as ** in Table 1). In addition to our resistance measurements being precise, the tight fits are also due to a physical reason ,as it is extremely hard for TMR to spuriously increase as it would require an increase in crystalline anisotropy to do so (*e.g.*, unlike in the coercivity data, there are no points above 1.0). These very promising results highlight the strong dependence of effective VCMA pMTJ dependence on crystalline quality of the active layers, which are being directly damaged by the microbeam in our experiment. These tight fits are predictive at this level, and can likely be used for application based modeling in the future.

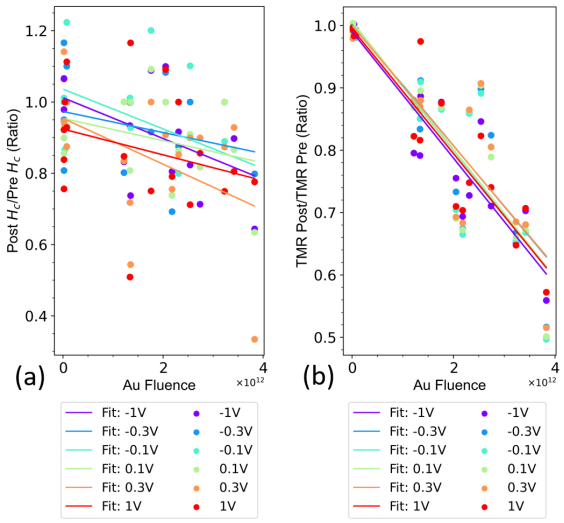

Fig. 5. Normalized coercivity and TMR as a function of fluence. (a), (b) show all measured data points $n = 18$ for all surviving deices, excluding control. The corresponding values for all fits shown are listed in Table 1.

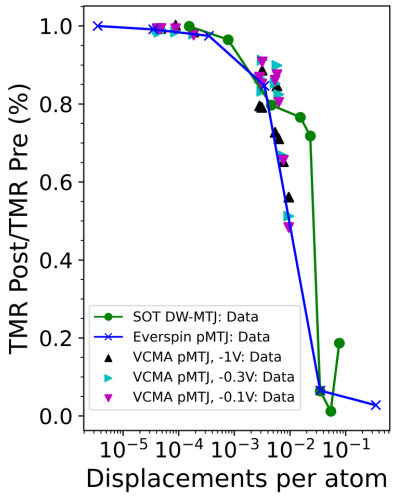

Fig. 6. Direct comparison to change in TMR as a function of dpa to our prior available data on different MTJ species. Specifically, the SOT fits are the same data shown in [7], and the pMTJ STT devices the same as in [8].

C. Benchmarking dpa changes with prior experiments

Lastly, the equivalent dpa values for every exposed device were computed relative to their starting values, and compared to other species of MTJs that have been evaluated for resilience to heavy ion irradiation. As shown in Fig. 6, while the variance in the dataset is higher than in previous experiments on SOT MTJs and STT pMTJs, our devices follow a similar response to prior experiments in terms of TMR degradation vs physical damage, which is expected given the similar experimental designs and device structure. In the case of the prior study on industry quality pMTJs [8], the fit is actually very tight. This result highlights that expressive VCMA functionality can

	Fit Parameters		Statistical Parameters		
	Applied V_b	Slope	Intercept	r^2 value	p-value
Coercivity Fits	$V_b = -1V$	$-5.72 \times 10^{-14}\ \frac{1}{\mathrm{ion/cm^2}}$	1.01	0.3	0.0183 *
	$V_b = -0.3V$	$-2.95 \times 10^{-14}\ \frac{1}{\mathrm{ion/cm^2}}$	0.973	0.098	0.2
	$V_b = -0.1V$	$-5.57 \times 10^{-14}\ \frac{1}{\mathrm{ion/cm^2}}$	1.04	0.274	0.025*
	$V_b = 0.1V$	$-3.12 \times 10^{-14}\ \frac{1}{\mathrm{ion/cm^2}}$	0.954	0.136	0.0132
	$V_b = 0.3V$	$-6.43 \times 10^{-14}\ \frac{1}{\mathrm{ion/cm^2}}$	0.955	0.217	0.05 *
	$V_b = 1V$	$-3.62 \times 10^{-14}\ \frac{1}{\mathrm{ion/cm^2}}$	0.924	0.0836	0.24
TMR Fits	$V_b = -1V$	$-1.02 \times 10^{-13}\ \frac{1}{\mathrm{ion/cm^2}}$	0.99	0.88	8.37×10^{-9} **
	$V_b = -0.3V$	$-9.73 \times 10^{-14}\ \frac{1}{\mathrm{ion/cm^2}}$	1	0.79	7.2×10^{-7} **
	$V_b = -0.1V$	$-1.02 \times 10^{-13}\ \frac{1}{\mathrm{ion/cm^2}}$	1	0.8	5.81×10^{-7} **
	$V_b = 0.1V$	$-1.036 \times 10^{-13}\ \frac{1}{\mathrm{ion/cm^2}}$	1.01	0.795	6.17×10^{-7}**
	$V_b = 0.3V$	$-9.66 \times 10^{-14}\ \frac{1}{\mathrm{ion/cm^2}}$	1	0.784	1.04×10^{-6} **
	$V_b = 1V$	$-1 \times 10^{-13}\ \frac{1}{\mathrm{ion/cm^2}}$	0.994	0.866	2.23×10^{-8}**

TABLE I
STATISTICAL CHARACTERIZATION OF POPULATION FITS FOR VCMA PMTJ DEVICES

be gained immediately for existing pMTJ species, and does not come at an additional cost in terms of radiation resilience.

IV. CONCLUSION

In conclusion, we have carefully studied the response of emerging VCMA pMTJ devices and found that they are intrinsically radiation resilient, and surprisingly, no more sensitive than standard pMTJ devices explored in other works. This result is encouraging, since the VCMA effect is heavily dependent on the quality of the perpendicular anisotropy. Since the anisotropy quality of the thin-films in a pMTJ device can be strongly affected based on even intermediate or low levels of disorder, it may be that devices at intermediate levels of fluence may show greater sensitivity to temperature or reduced endurance. These questions suggest that additional investigation on the reliability of these devices in those contexts may be worthwhile. In addition, since some of the current fluence to coercivity relationships are statistically insignificant, additional, higher-resolution field measurements can be taken on newly irradiated VCMA pMTJ devices to establish a more complete predictive model.

REFERENCES

[1] J. Slaughter, K. Nagel, R. Whig, S. Deshpande, S. Aggarwal, M. DeHerrera, J. Janesky, M. Lin, H.-J. Chia, M. Hossain *et al.*, "Technology for reliable spin-torque MRAM products," in *2016 IEEE International Electron Devices Meeting (IEDM)*, February 2017, pp. 21.5.1–21.5.4.

[2] W. Kang, Y. Ran, Y. Zhang, W. Lv, and W. Zhao, "Modeling and exploration of the voltage-controlled magnetic anisotropy effect for the next-generation low-power and high-speed mram applications," *IEEE Transactions on Nanotechnology*, vol. 16, no. 3, pp. 387–395, 2017.

[3] N. Zogbi, S. Liu, C. H. Bennett, S. Agarwal, M. J. Marinella, J. A. C. Incorvia, and T. P. Xiao, "Parallel matrix multiplication using voltage-controlled magnetic anisotropy domain wall logic," *IEEE Journal on Exploratory Solid-State Computational Devices and Circuits*, vol. 9, no. 1, pp. 65–73, April 2023.

[4] Y. Shao, C. Duffee, E. Raimondo, N. Davila, V. Lopez-Dominguez, J. A. Katine, G. Finocchio, and P. K. Amiri, "Probabilistic computing with voltage-controlled dynamics in magnetic tunnel junctions," *Nanotechnology*, vol. 34, no. 49, p. 495203, 2023.

[5] Y. Shao, N. Davila, F. Ebrahimi, J. A. Katine, G. Finocchio, and P. Khalili Amiri, "Reconfigurable physically unclonable functions based on nanoscale voltage-controlled magnetic tunnel junctions," *Advanced Electronic Materials*, vol. 9, no. 8, p. 2300195, 2023.

[6] E. A. Montoya, J.-R. Chen, R. Ngelale, H. K. Lee, H.-W. Tseng, L. Wan, E. Yang, P. Braganca, O. Boyraz, N. Bagherzadeh *et al.*, "Immunity of nanoscale magnetic tunnel junctions with perpendicular magnetic anisotropy to ionizing radiation," *Scientific reports*, vol. 10, no. 1, June 2020, art. no 10220.

[7] C. H. Bennett, T. P. Xiao, T. Leonard, X. Zhan, R. Gearba-Dolocan, J. Young, G. Vizkelethy, E. Bielejec, D. Hughart, M. Marinella, and J. A. Incorvia, "Radiation response of domain-wall magnetic tunnel junction logic devices," *IEEE Transactions on Nuclear Science*, pp. 1–1, 2023.

[8] T. P. Xiao, C. H. Bennett, F. B. Mancoff, J. E. Manuel, D. R. Hughart, R. B. Jacobs-Gedrim, E. S. Bielejec, G. Vizkelethy, J. Sun, S. Aggarwal *et al.*, "Heavy-ion-induced displacement damage effects in magnetic tunnel junctions with perpendicular anisotropy," *IEEE Transactions on Nuclear Science*, vol. 68, no. 5, pp. 581–587, February 2021.

[9] Y. Shao, V. Lopez-Dominguez, N. Davila, Q. Sun, N. Kioussis, J. A. Katine, and P. Khalili Amiri, "Sub-volt switching of nanoscale voltage-controlled perpendicular magnetic tunnel junctions," *Communications Materials*, vol. 3, no. 1, p. 87, 2022.

[10] J. F. Ziegler, M. D. Ziegler, and J. P. Biersack, "SRIM–the stopping and range of ions in matter (2010)," *Nuclear Instruments and Methods in Physics Research Section B: Beam Interactions with Materials and Atoms*, vol. 268, no. 11-12, pp. 1818–1823, June 2010.